Journal of Materials Chemistry A

Accepted Manuscript

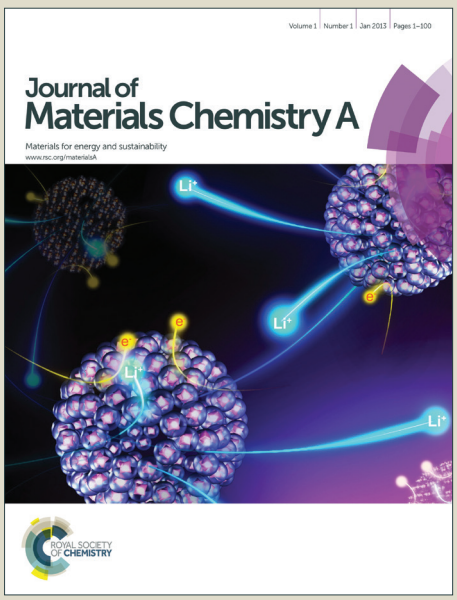

ROYAL SOCIETY OF CHEMISTRY

www.rsc.org/materialsA

Journal of Materials Chemistry A

RSCPublishing

PAPER

On the electrochemical origin of the enhanced charge acceptance of lead-carbon electrode†

Cite this: DOI:

Wenli Zhang[a], Haibo Lin [a,b*], Haiyan Lu[a*], Dechen Liu[a], Jian Yin[a], Zheqi Lin[a]

Received
Accepted

DOI:

www.rsc.org/

Bi-functional electrode materials, composed with capacitive activated carbon (AC) and battery electrode material, possess higher power performance than traditional battery electrode materials. Negative electrodes of lead acid battery with AC additives (lead-carbon electrode), compared with traditional lead negative electrode, is of much better charge acceptance, and is suitable for the energy storage in hybrid electrical vehicles. In this paper, we discussed the electrochemical processes on AC in lead-carbon electrode. In the charge process of lead-carbon electrode, lead electrodeposits on AC at higher potentials than the open circuit potential of lead, and the large surface area of AC provides extra active sites for lead electrodeposition and the growth of electrochemical active surface area of lead. Namely, AC acts as electron bumper and electron distributor in the charge process of lead-carbon electrode. Most importantly, the hydrogen evolution reaction (HER) on AC is prohibited by the reversible hydrogen adsorption at high charge rates, meanwhile the adsorbed hydrogen contributed to the charge process.

Introduction

Hybrid electrical vehicle (HEV) can effectively enhance the efficiency of energy utilization, which reduces the environmental pollution and retards the crisis of energy deficiency.[1] Nevertheless, supercapacitors are restricted by their low energy densities,[2] and traditional rechargeable batteries are restricted by their low power densities,[3] which is unsuitable for the application as energy storage module in HEVs.[4] Hence the development of battery with enhanced power performance is of great significance. Despite facing the challenge of advanced rechargeable batteries, the oldest rechargeable battery, lead acid battery, is still the most frequently used rechargeable batteries worldwide.[5] Beneficial to the characteristics of low price and good safety, lead acid battery has gained vast application in traditional automobile applications (start, light and ignition), and possesses great value in the potential application in HEVs.[6] Technological innovation makes lead acid battery always be an impetus in electrical energy storage market.[7]

The negative active material (NAM) of lead acid battery is of low surface area (*ca.* 0.7 m^2 g^{-1} vs. *ca.* 5 m^2 g^{-1} of positive active material), and is easily sulfated under the operation of partial state of charge (SoC) resulting in low charge acceptance of negative electrode, which is the restriction of lead acid battery in renewable energy storage and HEV applications. In recent years, the construction of bi-functional electrode materials composed with capacitive activated carbon (AC) and battery electrode materials has attracted researchers worldwide. The addition of a small amount AC in the battery electrode material makes the battery possess high power density without losing energy density apparently.[8] The lifespan and charge acceptance of a lead acid battery with lead-carbon electrode has been greatly enhanced under the operation of high rate partial state of charge (HRPSoC, operational condition of HEV), which almost perfectly solved the sulfation problem of lead negative electrode in such operation conditions.[9] The effects of AC in a lead-carbon electrode are always phenomenologically regarded as capacitive contribution, increase of conductivity, steric hindrance and electrocatalysis effect etc.[10-12] However, there is no clear evidence that which effect is dominating. The clarification of the functions of AC in lead-carbon electrode will promotes the development of lead-carbon battery.

P.T. Moseley supposed that if the energy used in HEVs application was all from the capacitive contribution of AC, the NAM should contain 25 wt.% high surface area AC.[11] As a matter of fact, the charge power of lead acid battery with only 2 wt.% AC in NAM was doubled in a very large range of SoC,[10] hence the role of AC is not merely capacitive contribution. Pavlov calculated the capacitive capacity of lead acid battery with AC in NAM. Results showed that the AC only provides 0.22% capacitive capacity of the total capacity in a HRPSoC cycle. Therefore, AC mainly improves the electrochemical process of lead electrode, which determines the charge acceptance. Based on this prominent effect of AC, D. Pavlov put forward that the lead electrode with AC additive should be termed "lead-carbon electrode".[12] We follow this terminology in this paper. Xiang et al. discovered that the potential of AC declines much slower than the lead component in lead-carbon electrode after pulse charge. Based on the above phenomenon,

he thought that the surplus electrons in AC are conducted to sites where electrochemical reduction of $PbSO_4$ occurred.[13] Due to the difficulty of separating the effects of AC and Pb, most researchers focused on the electrical performances of lead-carbon electrode, however, the effect of AC in lead-carbon electrode is of more significance.[14] The elaboration of the role of AC in lead-carbon electrode will help us design more effective lead-carbon architectures and instruct the production process of lead-carbon battery. Heretofore, the effects of AC on charge process of lead-carbon electrode are not very clear.

Herein, the electrochemical contributions of AC on charge process of lead-carbon electrode have been discussed. Experimental results demonstrate that AC contributes little capacitive capacity in the charge process, and it is the electrodeposition of Pb on the surface of AC that dominates the charge process of lead-carbon electrode. Besides, the hydrogen evolution reaction (HER) on AC was prohibited by the reversible hydrogen adsorption at high charge rates, and the adsorbed hydrogen contributed to the charge process. A charge mechanism of AC in lead-carbon electrode was also proposed in this paper based on the above results.

Experimental

Preparation of working electrode

Electrolytic lead plate (working area of 1×1 cm^2, purity > 99.99%) was served as the Pb electrode. Firstly, the Pb electrode was polished with emery paper to a mirror surface. Then, it was rinsed orderly with acetone and deionized water. Finally, the non-working surfaces of Pb electrode were sealed with epoxy resin. A Pb/AC electrode with excessive AC was designed to simulate the electrochemical process of AC in lead-carbon electrode (See Supporting Information, Fig. S1). The Pb/AC electrode was assembled by pressing the AC film on the surface of Pb electrode. The loading mass of AC film is 4 mg cm^{-2}. Deionized water and analytical grade reagent were used in all experiments. AC used in this experiment is a commercial carbon material for supercapacitors (YP-50F) (Kuraray, Japan). Detail properties of this kind of AC are listed in Table S1.

Characterization

The electrochemical characterizations of Pb and Pb/AC electrodes were carried out on a PARSTAT 2273 electrochemical wokstation (Princeton Applied Research, USA). A Ti/Pt electrode (2 cm × 2 cm) was used as the counter electrode. A mercurous sulfate electrode (MSE, $Hg/Hg_2SO_4/K_2SO_4$ (saturated), 0.658 V vs. SHE) was used as the reference electrode. Before all the electrochemical tests, the Pb and Pb/AC electrodes were polarized at -1.2 V for 20 min to eliminate the oxides on Pb surface. Galvanostatic charge-discharge (GCD) tests were carried out on a BTS system (Neware, China). The positive electrode was a pasted PbO_2 electrode (3 mm × 30 mm ×30 mm) with steady potential of 1.075 V. The Pb and Pb/AC electrodes were served as the negative electrode. Energy dispersive spectroscopy (EDS) and element distribution map were obtained by the combination of SU8020 scanning electron microscope (SEM) (Hitachi, Japan) and Quantax energy dispersive spectrometer (Bruker, Germany). All the electrochemical experiments were carried out in an aqueous solution of 5.0 mol L^{-1} H_2SO_4.

Results and discussion

For the faradaic process of a lead electrode, the charge process corresponds to the reduction of $PbSO_4$ and the discharge process corresponds to the oxidation of Pb (Eq. (1)).

$$PbSO_4 + H^+ + 2e^- \underset{discharge}{\overset{charge}{\rightleftharpoons}} Pb + HSO_4^- \quad (1)$$

The GCD of Pb and Pb/AC electrode was tested in the potential range from -0.7 V to -1.3 V at current density of 5.0 mA cm^{-2} (Fig. 1a and 1b).

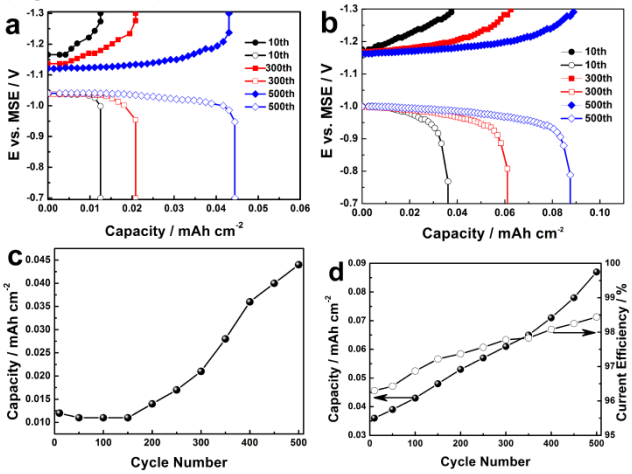

Fig. 1. GCD curves of (a) Pb electrode and (b) Pb/AC electrode at charge-discharge current density of 5.0 mA cm^{-2}; (c) Dependence of discharge capacity of Pb electrode on cycle number; (d) Dependence of discharge capacity and current efficiency of Pb/AC electrode on cycle number.

On one hand, the current efficiency of Pb electrode was very close to 100% and the current efficiency of Pb/AC electrode maintained at very high values from 96% to 99% (Fig. 1d), which indicates that the hydrogen evolution reaction on AC was unobvious. On the other hand, with the increase of cycle number, both the faradaic capacity of two electrodes increased and at the same cycle number the faradaic capacity of Pb/AC electrode was much higher than that of Pb electrode. The initial faradaic capacity of Pb electrode was 0.011 mAh cm^{-2}, and the faradaic capacity of Pb electrode at the 500th cycle was 0.044 mAh cm^{-2}. On contrast, the initial faradaic capacity of the Pb/AC electrode was 0.036 mAh cm^{-2}, and the faradaic capacity of Pb/AC electrode at 500th cycle was 0.087 mAh cm^{-2}. The above results reveal that the enhanced faradaic capacity of Pb/AC electrode could be attributed to the faradaic reaction on AC.

It is generally acknowledged that AC possesses almost no capacitive capacity and the main reaction occurring on AC is the hydrogen evolution reaction (HER) in the charge potential range of a lead electrode.[15] Since the capacitive potential window of AC (Fig. S2) is more positive than the open circuit potential (OCP) of Pb (-1.05 V) (Fig. S3a), HER occurs on AC

in the charge potential range of Pb/AC electrode (from -1.1 V to -1.3 V) (Fig. S3b). However, the high current efficiency of Pb/AC electrode indicates that the HER on AC is unobvious at a current density of 5.0 mA cm^{-2} (1.25 A g^{-1} vs. mass of AC). The reason for the high current efficiency was explained in the following.

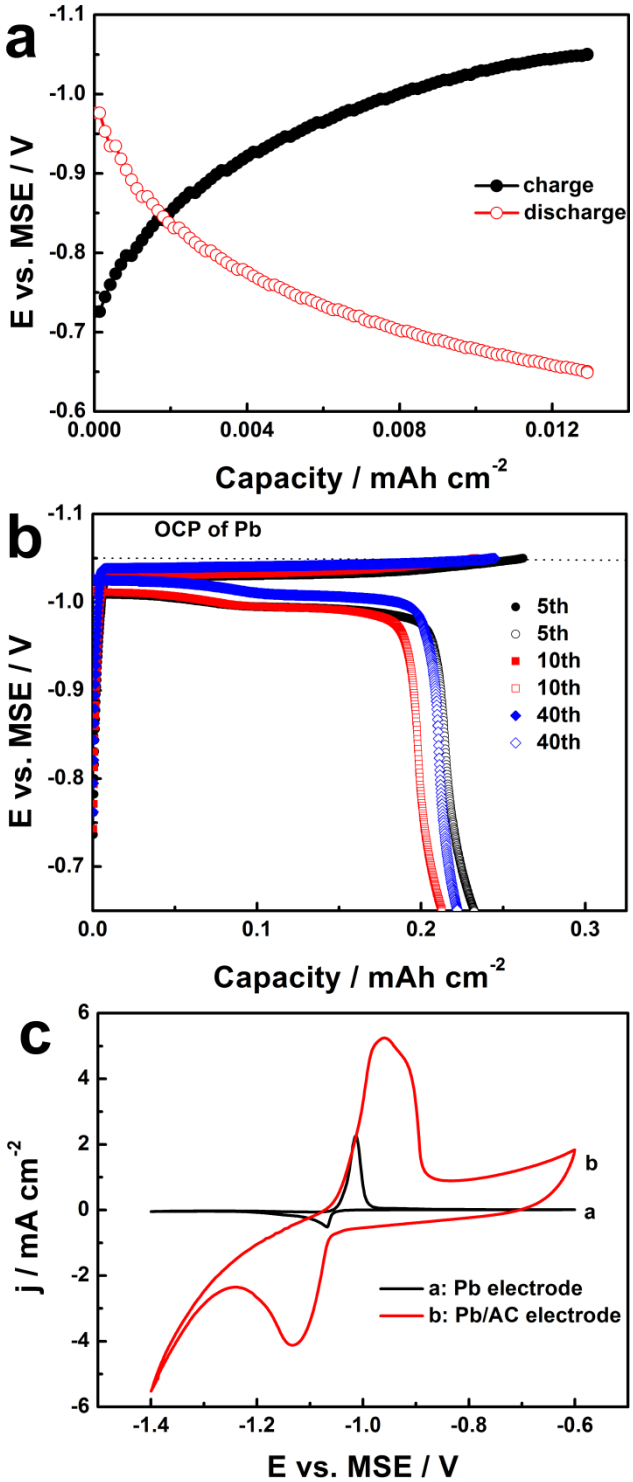

Fig. 2. GCD curves Pb/AC electrode at charge-discharge current density of 0.5 mA cm^{-2} in the potential range of -0.65 to -1.05 V (a) before and (b) after 500 GCD cycles at 5 mA cm^{-2}; (c) Cyclic voltammograms of Pb electrode and Pb/AC electrode at 1 mV s^{-1} after 500 GCD cycles at 5 mA cm^{-2}.

The GCD performances of the Pb/AC electrode in the potential range from -0.65 V to -1.05 V at 0.5 mA cm^{-2} were tested before and after 500 GCD cycles at 5.0 mA cm^{-2} (Fig. 2a and 2b).

The GCD performances of the Pb/AC electrode in the potential range from -0.65 V to -1.05 V at 0.5 mA cm^{-2} were tested before and after 500 GCD cycles at 5.0 mA cm^{-2} (Fig. 2a and 2b). Results show that the Pb/AC electrode only exhibited capacitive behavior with a capacity of *ca.* 0.013 mAh cm^{-2} (3.25 mAh g^{-1} vs. mass of AC) before cycling (Fig. 2a). However, the GCD curve changed greatly after 500 GCD cycles. At the very beginning of the charge process the potential dropped sharply, which was the capacitive behavior and was of small capacity. Then, the charge curve displayed a "plateau" (Fig. 2b), which is a sign of typical faradaic reaction,[16] where electricity is transformed into chemical energy. Since in the GCD test mode of electrochemical energy storage materials, the potential of supercapacitor electrode material changes linearly as time goes by, but a battery electrode material charges and discharges in a relatively unchanged potential range (plateau) where faradaic reaction occurs. The faradaic capacity was *ca.* 0.225 mAh cm^{-2} (56.25 mAh g^{-1} vs. mass of AC). Multiple GCD curves demonstrate that this kind of faradaic reaction, occurring at potentials more positive than the OCP of Pb, was of high reversibility. On the contrary, the Pb electrode showed no faradaic capacity in the same potential range (Fig. S4). The faradaic capacity of Pb/AC electrode at potentials more positive than the OCP of Pb originates from the deposition of Pb on AC in the cycling process, which results in the formation of AC·Pb composite (Eq. (2)).

$$AC + PbSO_4 + H^+ + 2e^- \rightarrow AC \cdot Pb + HSO_4^- \quad (2)$$

And the AC·Pb composite can be charged at potentials more positive than the OCP of Pb. Hence, in the charge process of lead-carbon electrode, the AC·Pb composite is charged preferentially. The formation of AC·Pb composite makes the lead-carbon electrode of high reversibility, which was demonstrated by cyclic voltammetry (Fig. 2c). After 500 GCD cycles, the Pb/AC electrode had both higher and much more symmetric peak currents, compared with Pb electrode with small peak and cathodic peak currents. The high reversibility of lead-carbon electrode results from addition of AC, which lowers the charge transfer resistance of the redox couple of $Pb/PbSO_4$. In addition, AC provides large surface area from both the out surface and inner pores for the deposition of Pb, which results in high electrochemical active surface area of Pb. So, the high electrochemical active surface area of Pb also accounts for the high electrochemical activity of lead-carbon electrode. The comparison of the cyclic voltammograms of Pb and Pb/AC electrode before and after 500 GCD cycles are shown in Fig. S5.

For the electrodes before cycling, the cathodic peak current of Pb/AC electrode was much higher than that of Pb

electrode, which is caused by the addition of AC. Since, AC provides large surface area for the electrodeposition of Pb, which results in high peak current densities. The peak currents of Pb/AC electrode after 500 GCD cycles were much higher than that of the Pb/AC electrode before 500 GCD cycles, which is caused by the gradual deposition of Pb on AC surface resulting in the enhancement of the electrochemical active surface area of Pb in the cycling process.

In our experiment, the lowered charge transfer resistance and the enhanced electrochemical active surface area were determined by electrochemical impedance spectroscopy (Fig. S6). After 500 GCD cycles, the charge transfer resistance of the $Pb/PbSO_4$ interface on Pb electrode was 132.5 Ω. While the charge transfer resistance of the $Pb/PbSO_4$ interface on Pb/AC electrode was only 19.49 Ω. The small charge transfer resistance of $Pb/PbSO_4$ on lead-carbon electrode, representing high electrochemical surface area of Pb, results from the gradually electrodeposited Pb on AC in the GCD cycles (Fig. S7). In summary, the AC in lead-carbon electrode can provides large electrochemical active surface area, and the AC·Pb formed on AC can be charged preferentially at more positive potentials than the OCP of Pb, where AC acts as electron bumper and can receive high charge current. Furthermore, with the AC·Pb composite charged completely, extra Pb electrodeposites on the surfaces of AC resulting in the growth of Pb surface and the enhancement of faradaic capacity. As a result of the large surface area of AC, AC can provide extra sites for the deposition of Pb, where AC acts as electron distributor. The above said two points enhanced the electron transfer reversibility of $Pb/PbSO_4$ redox couple in lead-carbon electrode.

In order to determine the formation of AC·Pb composite on AC in the cycling process, the AC film on Pb/AC electrode (at discharged state) cycled 500 GCD cycles was torn down to carry out XRD, EDS and element distribution map analysis. Fig. 3 shows the EDS, SEM and the element distribution map of Pb and S.

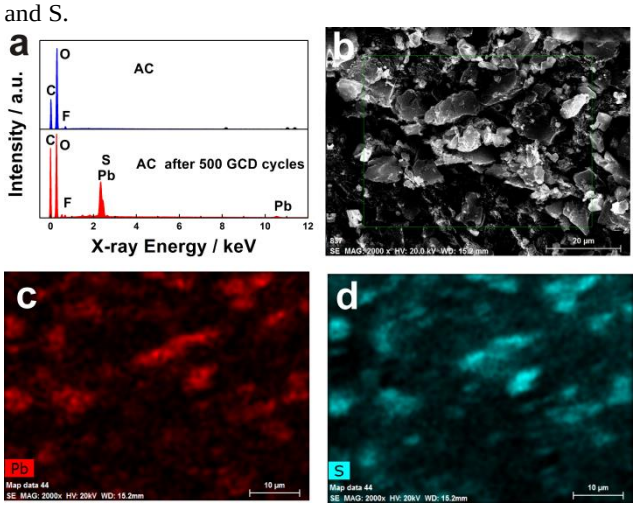

Fig. 3. (a) EDS spectra, (b) SEM image and element distribution map (Pb (c), S (d)) of AC film torn down from Pb/AC electrode (at discharge state) after 500 GCD cycles at 5.0 mA cm^{-2}.

EDS results show that after 500 GCD cycles the Pb deposited on the surface of AC with accompany of S (Fig. 3a). The element distribution map shows that the element of Pb and S located at the same position on AC (Fig. 3c and 3d), which indicates that the discharged state of Pb element on AC is in the form of $PbSO_4$, which is in accordance of the GCD and CV analysis. The XRD results also demonstrated the existence of $PbSO_4$ (Fig. S8). The above results show that the AC in lead-carbon electrode promotes the electron transfer reversibility of the $Pb/PbSO_4$ redox couple via the formation of AC·Pb composite. Hence the preparation of AC·Pb composite with high surface area which adapts to the lead-acid chemistry, the proper pore size and pore size distribution, is of great research importance.

The HER on the negative electrode has great influence on the energy storage efficiency of rechargeable battery.[17] HER not only lowers the current efficiency but also destroys the architecture of pasted type electrodes.[12] Hence the factors influencing HER should be carefully studied. In our experiment, the HER on the AC was investigated by cyclic voltammetry and GCD. The cyclic voltammetry was carried out at 1, 5, 10 and 20 mV s^{-1}, respectively (Fig. 4a).

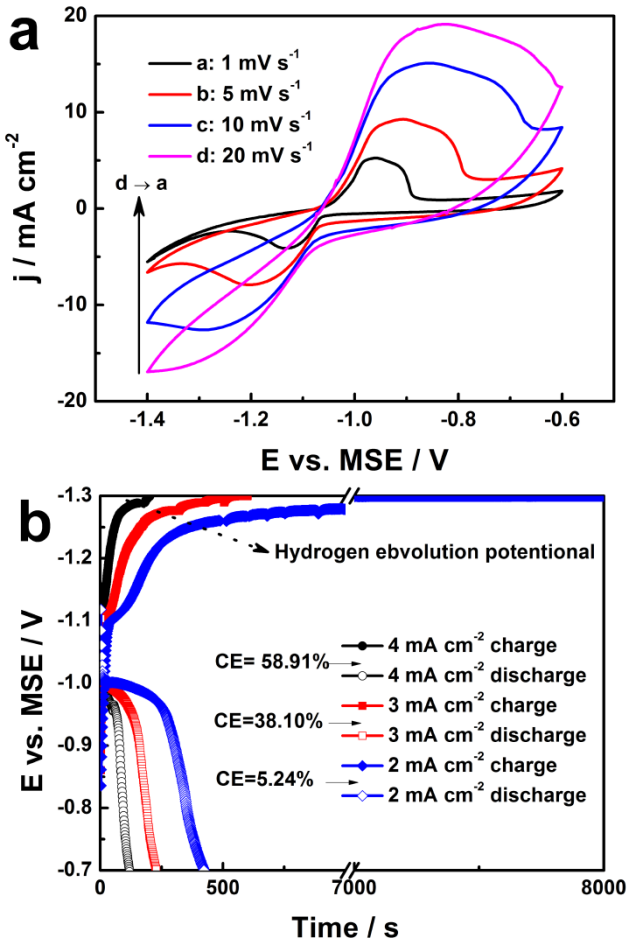

Fig. 4. (a) Cyclic voltammograms of Pb/AC electrode at 1, 5, 10 and 20 mV s^{-1} after 500 GCD cycles at 5 mA cm^{-2}; (b) GCD curves of Pb/AC electrode at different current densities after 500 GCD cycles at 5.0 mA cm^{-2}.

The cyclic voltammograms at different scan rates correspond to different charge-discharge rates. When the cyclic voltammetry was taken at 20 mV s^{-1}, the HER on Pb/AC electrode was not obvious even at the potential of -1.4 V; and the cathodic peak relating to the reduction of $PbSO_4$ was shifted to more negative potentials compared with CV taken at lower scan rates. However, the cathodic peak of the reduction of $PbSO_4$ and the irreversible hydrogen evolution curve were separated when the scan rate was lowered to 1 mV s^{-1}. The cathodic peak of the reduction of $PbSO_4$ located from -1.07 V to -1.25 V, while the irreversible hydrogen evolution curve located from -1.25 V to -1.4 V. This means that at a low charge rate, in the potential range of -1.25 V to -1.4 V, the main reaction is hydrogen evolution, which results in a low current efficiency.

The above results show that if the AC in lead-carbon electrode is charged at high current densities, the HER on AC is unobvious even at very low potentials and the main reaction occurring on AC is the reduction of $PbSO_4$ (Eq. (2)). Additionally, there is another reaction, the reduction of protons. The proton is mainly reduced and exists in the form of adsorbed hydrogen via Volmer reaction (Eq. (3)) at high charge current densities, since there is not enough time for the separation of hydrogen gas from AC surface via Heyrovsky reaction (Eq. (4)) or via Tafel reaction (Eq. (5)) (Fig. S9).

$$AC + H^+ + e^- \rightarrow AC \cdot H \quad (3)$$

$$AC \cdot H + H^+ + e^- \rightarrow AC + H_2 \quad (4)$$

$$AC \cdot H + AC \cdot H \rightarrow 2AC + H_2 \quad (5)$$

So the current efficiency of Pb/AC electrode is high (Fig. 1d) when the AC is charge-discharged at a relatively high current density of 5 mA cm^{-2} (1.25 A g^{-1}). At low charge current densities, both the reaction of Eq. (3), (4) and (5) on AC has enough time for the separation of hydrogen gas from the surface of AC, which is the reason for the low current efficiency at low charge-discharge current densities (Fig. 4b).

The above results explain the high current efficiency in Fig. 1. The results are helpful in the design of lead-carbon batteries for different applications, where different cut off potential upon charge should be applied. For instance, in the operational condition of HRPSoC for HEVs, the charge-discharge current is always high, the HER on AC is unobvious. While experiencing the full charge of a lead-carbon battery used in HEV with low current density for the purpose of energy recovery, the NAM of lead-carbon battery will be destroyed.[12] If the lead-carbon battery was used in the hours-long energy storage applications, such as renewable energy storage and load levelling in a smart grid, the cut off potential upon charge should be restricted relatively high to avoid excessive hydrogen evolution.

Based on the above experimental results, the effects of AC on the charge process of lead-carbon electrode were proposed (illustrated in Fig. 5).

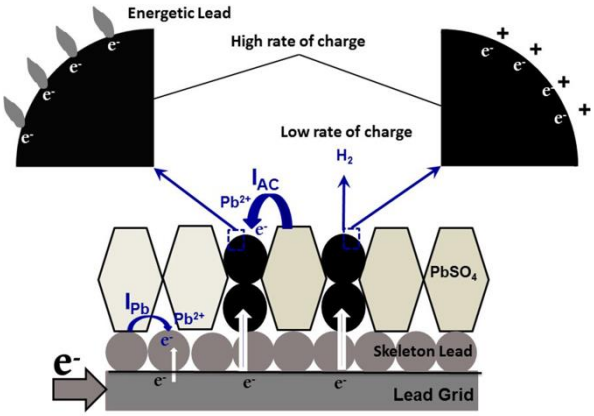

Fig. 5. Proposed charge mechanism of lead-carbon electrode.

(a), AC receives capacitive current, where capacitive capacity is very small;

(b), The potential of lead-carbon electrode is polarized to relatively negative values, where $PbSO_4$ is reduced to Pb on two surfaces, namely, the surface of Pb and the surface of AC. Because AC possesses large surfaces area and Pb can be deposited on AC at more positive potentials than that on Pb surface, AC can receive high faradaic current density ($I_{AC} > I_{Pb}$), where AC acts as electron bumper. Meanwhile, the large surface area of AC can provide active sites for the growth of electrochemical active surface area of Pb, thus providing more directions for the charge-current to distribute, where AC acts as electron distributor (like the role of grids in the negative plate in lead acid battery). Besides, the reduction of H^+ on the surface of AC coexists with the reduction of $PbSO_4$ in the charge process of a lead-carbon electrode.

(c), HER, the inevitable side reaction in the charge process of lead-carbon electrode, is controlled by the charge rate. The HER on the AC in lead-carbon electrode is obvious when the charge current is low, and the HER on AC is unobvious when the charge current density is high.

Conclusions

Presented here is an ongoing research focusing on the effects of AC on the charge mechanism of lead-carbon electrode. Results show that the capacitive contribution of AC is little, and it is the electrodeposition of Pb on the surface of AC that dominates the charge process of lead-carbon electrode. Since AC has large surfaces area and Pb can be deposited on AC at more positive potentials than that on Pb surface, AC can receive high faradaic current, where AC acts as electron bumper. Meanwhile, the large surface area of AC provides active sites for the growth of Pb branches, thus providing more directions for current distribution, where AC acts as electron distributor. Besides, the HER on the AC in lead-carbon electrode is unobvious when the charge current density is large, where H^+ is reduced mainly in the form of adsorbed protons on the surface of AC, which also contributes to the charge capacity. The above three points are the main electrochemical contributions of AC for the enhanced charge acceptance of lead-carbon electrode.

Acknowledgements

Financial support provided by the key project in Jilin Province (No. 20126010) is greatly acknowledged.

Notes and references

[a] *College of Chemistry, Jilin University, Changchun 130012, China*.
[b] *Key Laboratory of Physics and Technology for Advanced Batteries of Ministry of Education, Jilin University, Changchun, 130012, China*.
* *Corresponding author. Tel.: +86 431 85155189; fax: +86 431 85155189 E-mail address:* lhb910@jlu.edu.cn *(H. Lin),* luhy@jlu.edu.cn *(H. Lu)*

† Electronic supplementary information (ESI) available: Fabrication of Pb/AC electrode, capacitive behavior investigation of AC, OCP transients of AC and Pb, Tafel plots of Pb and Pb/AC electrode, GCD curves of Pb electrode in the potential range from -0.7 to -1.05 V after 500 GCD cycles at 0.5 mA cm^{-2}, GCD curves of Pb and Pb/AC electrode before and after 500 GCD cycles at 5 mA cm^{-2}, EIS spectra and the related equivalent circuits with simulated values of electrical elements for Pb and Pb/AC electrodes at OCP after 500 GCD cycles at 5 mA cm^{-2}, XRD patterns of AC and AC cycled after 500 GCD cycles at 5 mA cm^{-2}, Chronoamperometry curves of Pb, Pb/$PbSO_4$, Pb/AC and Pb/AC/$PbSO_4$ electrodes at different potentials.

1 N. Armaroli and V. Balzani, Energy Environ. Sci., 2011, **4**, 3193–3222.
2 M. Winte and R.J. Brodd, Chem. Rev. 2004, **104**, 4245−4269.
3 D.W. Wang, F. Li, M. Liu, G.Q. Lu and H.M. Cheng, Angew. Chem. Int. Ed., 2008, **47**, 373–376.
4 C.E. Holland, J.W. Weidner, R.A. Dougal and R.E. White, J. Power Sources, 2002, **109**, 32–37.
5 M.R. Palac ń, Chem. Soc. Rev., 2009, **38**, 2565–2575.
6 (a) D. Pavlov, Lead-Acid Batteries: Science and Technology, Elsevier B.V., Amsterdam, 2011; (b) D.A.J. R, P.T. Moseley, J. Garche and C.D. Parker, Valve-regulated Lead Acid Batteries, Elsevier B.V., Amsterdam, 2004; (c) J. Garche, Phys. Chem. Chem. Phys., 2001, **3**, 356–367.
7 (a) R. Shapira, G.D. Nessim, T. Zimrin and D. Aurbach, Energy Environ. Sci., 2013, **6**, 587–594; (b) M.G. Verde, K.J. Carroll, Z.Wang, A. Sathrum and Y.S. Meng, Energy Environ. Sci., 2013, **6**, 1573–1581; (c) L.X. Ding, F.L. Zheng, J.W. Wang, G.R. Li, Z.L. Wang and Y.X. Tong, Chem. Commun., 2012, **48**, 1275–1277; (d) Y. Kwon, H. Lee and J. Lee, Nanoscale, 2011, **3**, 4984–4988; (e) P.N. Bartlett, T. Dunford and M.A. Ghanem, J. Mater. Chem., 2002, **12**, 3130–3135; (f) X. Jiang, Y. Wang, T. Herricks and Y. Xia, J. Mater. Chem., 2004, **14**, 695–703.
8 (a) S.L. Candelaria, R. Chen, Y.-H. Jeong and G. Cao, Energy Environ. Sci., 2012, **5**, 5619–5637; (b) V. Etacheri, D. Sharon, A. Garsuch, M. Afri, A.A. Frimer and D. Aurbach, J. Mater. Chem. A, 2013, **1**, 5021–5030; (c) H.S. Choi, J.H. Im, T. Kim, J.H. Park and C.R. Park, J. Mater. Chem., 2012, **22**, 16986–16993; (d) Y. Wang, P. He and H. Zhou, Energy Environ. Sci., 2011, **4**, 4994–4999; (e) A.D. Pasquier, I. Plitz, J. Gural, F. Badway, G.G. Amatucci, J. Power Sources, 2004, **136**, 160–170; (f) X. Hu, Z. Deng, J. Suo, Z. Pan, J. Power Sources, 2009, **187**, 635–639; (g) D. Pavlov and P. Nikolov, J. Electrochem. Soc., 2012, **159**, A1215–A1225.
9 (a) F. Cheng, J. Liang, Z. Tao and J. Chen, Adv. Mater., 2011, **23**, 1695–1715; (b) L. Zhao, B. Chen and D. Wang, J. Power Sources, 2013, **231**, 34–38; (c) L. Zhao, B. Chen, J. Wu and D. Wang, J. Power Sources, 2014, **248,** 1–5; (d) D. Pavlov, P. Nikolov and T. Rogachev, J. Power Sources, 2011, **196**, 5155–5167.
10 M. Fern ández, J. Valenciano, F. Trinidad and N. Muñoz, J. Power Sources, 2010, **195**, 4458–4469.
11 P.T. Moseley, J. Power Sources, 2009, **191**, 134–138.
12 D. Pavlov and P. Nikolov, J. Power Sources, 2013, **242**, 380–399.
13 J. Xiang, P. Ding, H. Zhang, X. Wu, J. Chen and Y. Yang, J. Power Sources, 2013, **241**, 150–158.
14 Z. Yang, J. Zhang, M.C.W. Kintner-Meyer, X. Lu, D. Choi, J.P. Lemmon and J. Liu, Chem. Rev., 2011, **111**, 3577–3613.
15 L.T. Lam and R. Louey, J. Power Sources, 2006, **158**, 1140–1148.
16 P. Simon, Y. Gogotsi and B. Dunn, Science, 2014, **343**, 1210−1211.
17 S. Malkhandi, B. Yang, A.K. Manohar, G.K.S. Prakash, and S.R. Narayanan, J. Am. Chem. Soc., 2013, **135**, 347−353.

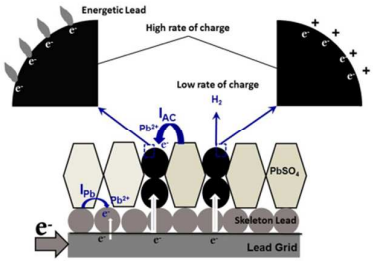

Electrochemical origins of the enhanced charge acceptance of lead-carbon electrode were investigated by various electrochemical methods.